Extended and accurate determination of the melting curves of argon, helium, ice (H_2O), and hydrogen (H_2)

Frédéric Datchi*
Université Pierre et Marie Curie, Physique des Milieux Condensés, T13, E4, B77, 4 Place Jussieu, 75252 Paris Cedex 05, France

Paul Loubeyre
SMPC/DPTA/DIF, CEA, 91681 Bruyères-le-Châtel, France
and Université Pierre et Marie Curie, Physique des Milieux Condensés, T13, E4, B77, 4 Place Jussieu, 75252 Paris Cedex 05, France

René LeToullec
Université Pierre et Marie Curie, Physique des Milieux Condensés, T13, E4, B77, 4 Place Jussieu, 75252 Paris Cedex 05, France
(Received 6 August 1999)

The melting curves of argon, helium 4, ice (H_2O), and hydrogen (H_2) have been measured from room temperature up to a maximum temperature of 750 K. This extends the previous determination of the melting lines of H_2 and He by nearly a factor of 2 in pressure. The experiments were carried out with a resistively heated diamond anvil cell. Improved accuracy with respect to previous determinations, when existing, was achieved by the use of an optical metrology which gives an *in situ* measurement of both the pressure and temperature of the sample. The melting lines of argon and H_2O are found to be well represented by the following Simon-Glatzel equations: $P=2.172\times10^{-4}T^{1.556}-0.21$ (argon) and $P=2.17+1.253[(T/354.8)^{3.0}-1]$ (H_2O). But the Simon-Glatzel form was found inadequate to reproduce the melting data of ^{4}He and H_2 over the whole temperature range. In the case of ^{4}He, this deviation from a Simon law is explained by the softening of the pair interaction with density. A Kechin equation is proposed for H_2: $T=14.025(1+P/0.0286)^{0.589}\exp(-4.6\times10^{-3}P)$. This form is in excellent agreement with all published experimental data for H_2 and interestingly predicts a maximum on the melting curve at 128 GPa and 1100 K.

I. INTRODUCTION

Melting is an important phase transition because it separates two different states of matter, solid and liquid. It is easy to observe and it covers the widest range of pressure and temperature among the first-order phase transitions. Hence melting is certainly the first measurement to be performed to explore the new *P-T* range now accessible with resistively or laser-heated diamond anvil cell (DAC). Change of slope, cusps, maximum on the melting curve can reveal subtle changes in the interactions of the system or differences between the properties of the fluid and the solid. Also, despite a vast literature on melting, fundamental questions such as the microscopic mechanisms of melting (surface melting, instability of the solid, importance of defects), the difficulty of calculations of the melting curve of real systems (the case of ideal systems interacting through simple pair potentials has been solved in the 1960s) or the evolution of melting to very high pressure are still actively debated.

He, H_2, and H_2O have already been the focus of great interest at high pressure for various reasons:[1] (1) Their electronic simplicity makes them the most amenable systems to a theoretical description and therefore they make reference experimental data to test *ab initio* calculations; (2) a very interesting evolution with pressure, respectively to a metal for hydrogen and to a ionic system for water, has been predicted; (3) their high *P-T* properties are essential input in the models of the jovian planets and their satellites. Up to now, the determination of the properties in the solid phase, at room temperature or below, has been achieved in DAC's whereas those in the liquid phase at high temperatures were obtained from shock waves. To bridge the *P-T* gap between these two methods of investigation and try and understand important differences in the properties of the dense solid and dense fluid phases of these simple molecular systems, it is important to couple high static pressures with high temperatures and obtain accurate data under such thermodynamic conditions. Few such attempts have been published in the literature because of the difficulty to perform accurate *P-T* determinations, or to keep the mechanical stability of the DAC at high temperature that is necessary to observe the melting equilibrium, or to limit the chemical reactivity of H_2 and H_2O under such conditions.

We present here extension in the *P-T* range and in the accuracy of the measurements of the melting curves of He, H_2O, and H_2. Their presentation in the same article should give a better confidence in the accuracy of our procedure and the analysis of their deviations from a regular evolution should appear more meaningful. The techniques used for these experiments are briefly presented in the experimental section (Sec. II). The melting curve of Ar is presented to validate our experimental procedure. Then the melting curves of the various systems are presented in different paragraphs of Sec. III and compared to the other determinations and calculations for He, H_2O, and H_2. The discussion of the data, Sec. IV, is focused on the validity of various melting

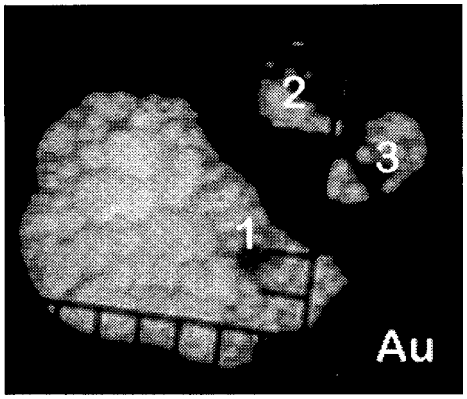

FIG. 1. Microphotograph of a H_2O sample at melting at 400 K. Three holes were drilled inside the gold liner isolating the sample from the rhenium gasket: (1) Large H_2O sample with a ruby ball; (2) $SrB_4O_7:Sm^{2+}$ powder in a smaller volume of H_2O; (3) ruby ball in H_2O. It can be observed that melting occurs simultaneously in the three holes.

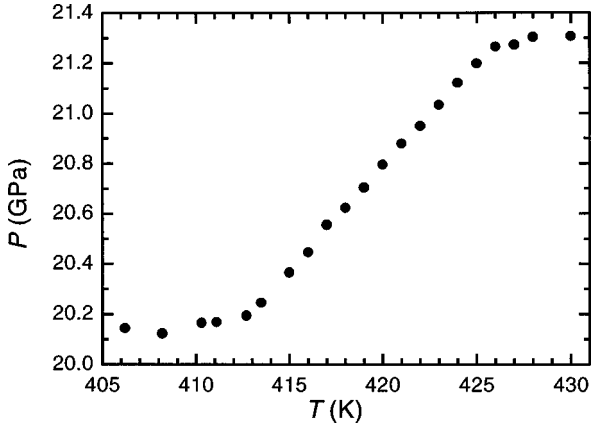

FIG. 2. Example of a quasi-isochoric scan in a ^4He sample at melting. The volume discontinuity at the transition leads to a pressure jump.

forms to reproduce the data and to extrapolate them. Some interesting trends are pointed out.

II. EXPERIMENTAL PROCEDURE

The present experiments used a diamond anvil cell that was specifically designed for high-temperature studies.[2] The body of this cell, including the diamond seats, is built out of ceramic materials that confine the high temperatures in the vicinity of the sample. A small resistive heater of spiral shape is attached to the metallic gasket (used to confine the sample) to allow heating of the sample. A power of 50 W is typically needed to reach a sample temperature of about 1000 K. The force on the moving piston is exerted by the inflation of a membrane under a helium pressure. The main advantage of this setup is to provide a very good mechanical stability while working at high temperatures: no drop of pressure is observed during heating, in contrast to other reported designs. Furthermore, the use of an external heater provides a good thermal stability, so that the conditions of pressure and temperature of the sample can be finely controlled and made stable in a short time. This allows an easy and accurate detection of the location of a phase transition such as melting.

Rhenium foils of 0.25-mm thickness served as gaskets. In the experiments on H_2 and H_2O, the samples were isolated from the rhenium gasket by a fine gold liner (other materials were also used in the case of H_2, as explained in Sec. III D), in order to prevent chemical reaction between the sample and rhenium. High-purity gases were loaded at room temperature using high-pressure loading techniques.

In the case of Ar, H_2O, and H_2, melting could be detected by direct visualization of the samples. The difference in the refractive index of the solid and fluid phase was large enough for a solid/fluid equilibrium to be observed up to the maximum temperature. Starting from the solid phase and keeping the load constant, we slowly increase the temperature of the sample. At the onset of melting, one or several small crystallites appear in equilibrium with the fluid (Fig. 1). When this equilibrium is stabilized, the measurements of pressure and temperature provide the location of the melting point. Pressure and temperature are then slowly raised in order to maintain the sample in this topology. This method allows a fine sampling of the melting line. In the case of helium though, the difference in the refractive index of the two phases is too small (e.g., $\Delta n/n \sim 0.33\%$ at 300 K)[3] to use this technique. Hence we carried out quasi-isochoric scans near the melting line (Fig. 2): starting from the solid phase, we increase the temperature by small steps. At melting, the pressure increases due to the volume discontinuity, up to the point where the solid phase has totally disappeared. The midpoint of such an isochore defines the melting point.

An important effort of this work was devoted to the improvement of the accuracy of high-pressure–high-temperature measurements in DAC's. Whereas reliable and precise methods exist to measure the pressure in a DAC at temperatures below 300 K, it is more difficult to precisely characterize both the pressure and temperature of the sample at higher temperatures. For instance, the use of the well-known ruby gauge[4] is made more and more difficult because of the fall in intensity and the broadening of the R_1 line. Besides, the exact knowledge of the sample temperature is important since the wavelength shift of the ruby line has a large temperature dependence. The measurement of the sample temperature is not trivial because large temperature gradients may exist in the DAC. For example, a difference as large as 160 K was observed in the present experiments between the temperature of the sample chamber (740 K) and the one measured with a thermocouple in contact with the gasket, 1 mm away from the sample. Therefore it is very important to perform an *in situ* measurement of both the pressure and temperature. This was achieved here by using the method described in a recent paper:[5] we measure the fluorescence of two optical sensors, ruby and $SrB_4O_7:Sm^{2+}$, placed inside the sample; pressure is deduced from the wavelength shift of the $^5D_0$-$^7F_0$ line of $SrB_4O_7:Sm^{2+}$ and temperature from the one of the ruby R_1 line. This is made possible because (i) the temperature dependence of the $SrB_4O_7:Sm^{2+}$ luminescence line is negligible,[40] and (ii) the temperature and pressure dependencies of the ruby line are uncoupled, as shown by numerous experiments. This method was indirectly validated by the very good reproducibility observed between different set of measurements obtained with different geometry of sample heating (see also Sec. III A).

We used a 1.3-m focal length Jarell-Ash spectrometer, equipped with a 1800-gr/mm grating and coupled to a $l\mathrm{N}_2^-$ cooled charge-coupled device detector from Princeton Instruments, that allowed measurements of the fluorescence line positions with a precision of the order of 5×10^{-3} nm. The accuracy of our *T-P* measurements is then usually better than ±3 K and ±0.05 GPa up to 600 K. At higher temperature, the fall in intensity and broadening of the lines make the measurements less accurate and we estimate our worst uncertainty to be ±15 K and ±0.2 GPa at 750 K. This method is unfortunately limited to about 750 K because of the rapid quenching of the luminescence of the two sensors around this temperature.[5] We want to stress that, although our DAC would allow us to perform experiments at higher pressures and temperatures than those reported here, we deliberately limited our experiments to this temperature region, in order to have good confidence and consistency in the accuracy of our measurements.

Figure 1 shows a microphotograph of a H_2O sample at melting near 400 K. As mentioned above, a gold liner was used to isolate the sample from the rhenium gasket. Chemically inert materials like Au are indeed required for H_2O and H_2 because of the high chemical reactivity of these elements at elevated pressures and temperatures. H_2O also reacted with the $SrB_4O_7:Sm^{2+}$ pressure gauge, resulting in the total dissolution of the sensor above 650 K (8.5 GPa). This was resolved by drilling three separate holes as shown in Fig. 1: a large one for observation of the water sample, a second smaller one with a borate sample in large relative amount, and a third one with a ruby ball. We checked that the samples in the three holes were at the same pressure. The measurements could then be carried out at higher temperature. The case of H_2 was more complicated, as discussed in Sec. III D.

III. DETERMINATION OF THE MELTING CURVES

A. Melting curve of argon: A test of the experimental method

Our main purpose in measuring the melting curve of argon was to test the techniques developed in this study. Argon was a good system because its melting pressure remains relatively low up to 1000 K ($P<9$ GPa), which presented no risk of failure for our DAC. Argon is also chemically inert so that reaction of the sample with surrounding elements (gasket, diamonds) was unlikely. Besides, numerous works had already reported determinations of the melting line of argon, which we could use as a test of our experimental procedure.

We carried out experiments on four different samples. For the first two experiments, a DAC made out of high-temperature steel was used instead of the ceramic DAC. This DAC was externally heated by a specially designed furnace that wrapped the whole cell. The highest temperature that could be reached with this setup was 590 K. Using the ceramic DAC, the determination was extended to 740 K. The importance of an *in situ* determination of temperature was well illustrated here, since for an identical temperature of the sample, the temperature measured with a thermocouple placed inside the gasket at about 1 mm away from the sample was very different, depending on the experimental setup used: it was only a few degrees larger with the large external furnace but was up to 160 K larger at 740 K in the ceramic DAC.

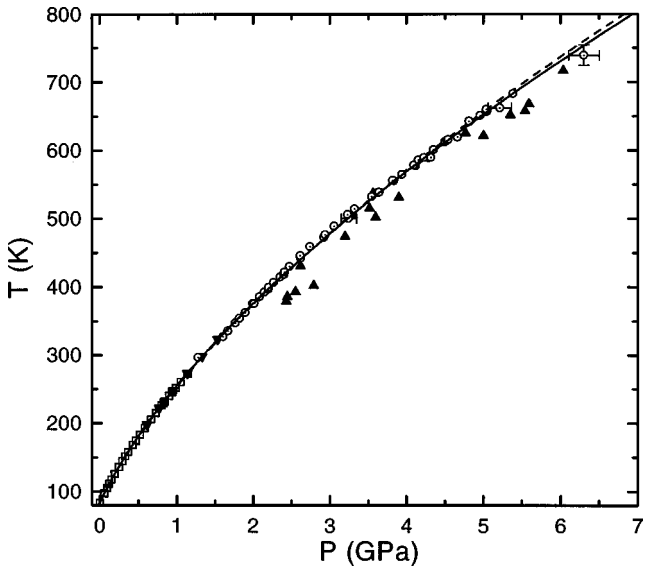

FIG. 3. Melting curve of argon. ⊙: this work; □: Hardy *et al.* (Ref. 6); ▼: Stishov *et al.* (Ref. 7); ▲: Zha *et al.* (Ref. 8) ——: $P=2.172\times10^{-4}T^{1.556}-0.21$; ––: $P=2.67348\times10^{-4}T^{1.522\,99}-0.229\,33$ (Ref. 6).

In total, over a hundred melting points were recorded between 1.28 GPa (296.5 K) and 6.3 GPa (739.5 K), with large regions of overlap between the different experiments. For clarity, only some of these points are gathered in Fig. 3 and Table I. The reproducibility between the different measurements is very good as one can infer from the weak dispersion of our data.

Numerous groups measured the melting line of argon in the 1960s and 1970s, mostly from the zero pressure melting point (83.78 K) up to 320 K.[41] They usually agree within the experimental uncertainties and are well represented by the Simon law fitted on Hardy, Crawford, and Daniels's very precise data:[6]

$$P=2.67348\times10^{-4}T^{1.522\,99}-0.229\,33. \tag{1}$$

Figure 3 shows this equation as well as the experimental data from Hardy, Crawford, and Daniels[6] and from Stishov and Fedosimov.[7] It can be seen that our measurements agree with those of Stishov and Fedosimov in the region of overlap and lie well in the extrapolation of all the low-pressure data points. At higher temperature, our data may be compared to those of Zha *et al.*[8] which approximately cover the same *P-T* range. These authors also used a resistive heating method in a diamond cell. They measured pressure with the ruby line and temperature with a thermocouple ''attached to the diamond.'' Up to 3.6 GPa, they could detect melting by visualization of the sample, but had to use an interference method at higher pressure. We note that the contrast was good enough in our experiments to visually detect melting up to the highest pressure studied (6.3 GPa). The dispersion in Zha *et al.*'s data is larger than in ours, indicating a poorer experi-

TABLE I. Experimental melting points of argon determined in this work. T_m in K and P_m in GPa.

T_m	P_m	T_m	P_m
296.5	1.28	532.0	3.54
326.9	1.61	538.6[a]	3.64[a]
335.6	1.67	538.7	3.64
347.4	1.77	555.7	3.84
354.1[a]	1.82[a]	555.8[a]	3.82[a]
354.2	1.82	564.4[a]	3.94[a]
362.6	1.89	577.2	4.12
375.6	1.99	578.4[a]	4.10[a]
375.9[a]	2.01[a]	586.2	4.16
385.7	2.08	589.0[a]	4.29[a]
392.6	2.14	589.5	4.23
397.1[a]	2.20[a]	589.9[a]	4.32[a]
399	2.20	601.6	4.35
406.6	2.27	612.8	4.50
414.8	2.35	615.2	4.53
418.2[a]	2.40[a]	616.1	4.55
421.7	2.41	619.8	4.67
430.3	2.47	642.7	4.82
442.6[a]	2.62[a]	643.0	4.82
446.2	2.61	651.5	4.96
459.2	2.74	657.2	5.04
472.8	2.92	657.5	5.05
476.5[a]	2.94[a]	660.2	5.04
489.1	3.05	662.4	5.22
500.2	3.25	683.1	5.38
506[a]	3.23[a]	739.5	6.30
514.3[a]	3.32[a]		

[a]Measurements that used the external furnace.

mental accuracy. They measured in average a lower melting pressure than we did but the two data sets show similar slopes.

Equation (1) can be seen to represent our data quite well, except at the highest pressures where it stands slightly outside of the estimated error bars. A least-square fit to both Hardy, Crawford, and Daniels's and present data leads to a slightly modified form, also plotted in Fig. 3:

$$P = 2.172 \times 10^{-4} T^{1.556} - 0.21. \quad (2)$$

Melting of argon was recently studied by Jephcoat and Besedin in a laser-heated DAC experiment.[9] The five melting points measured between 26 and 47 GPa are plotted in Fig. 4 and compared to Eqs. (1) and (2). The error bars associated to the laser heating data are larger than the difference between the two relations inside this *P-T* range. However, this experiment indicates that the melting line of argon should follow a Simon law at least up to 50 GPa. We also note that calculations by Zha *et al.*[8] of the argon melting line based on the exponential-6 pair potential agree very well with the present data.

B. Melting curve of He: Exploration of a large domain in reduced unit

The study of melting of helium is interesting in several aspects. First, helium is the atom with the simplest electronic

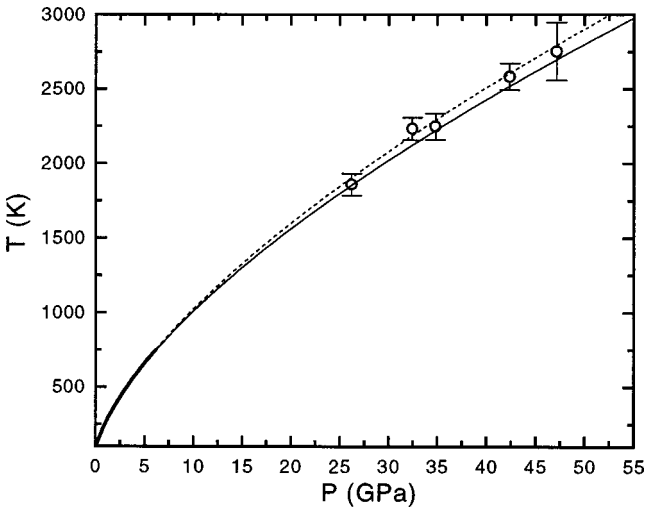

FIG. 4. Melting curve of argon, showing the data from the laser-heating experiment by Jephcoat *et al.* (Ref. 9). The thick line shows the melting line obtained in this work. The full and dashed lines represent, respectively, the equations $P = 2.172 \times 10^{-4} T^{1.556} - 0.21$ (this work) and $P = 2.673\,48 \times 10^{-4} T^{1.522\,99} - 0.229\,33$ (Ref. 6).

structure, which makes it a model system for calculations. Second, according to the law of corresponding states, helium is the system giving access to the largest *P-T* range in reduced units. Third, several calculations have predicted a hcp to bcc phase transition along the melting line.[10] Previous studies showed that cusps on the melting curve at 15 and 300 K corresponded to the fcc-hcp-liquid triple points, and it is expected that the hcp-bcc transition produces a similar accident.

A single experiment was performed on helium. The ten melting points obtained by the isochoric method described in Sec. II are gathered in Fig. 5 and Table II. They cover a pressure range from 13.8 to 41.2 GPa, corresponding to melting temperatures between 326.2 and 608 K. This experiment was prematurely stopped by the failure of the membrane used to generate the force on the piston of the DAC. We also noticed a trend of He embrittlement of the diamond anvils at high *P-T* which might make the extension of the measurements of the melting curve more difficult.

The melting line of ^{4}He was previously investigated up to the highest pressure of 24 GPa by Vos, van Hinsberg, and Schouten.[11] Their data may be compared to the present ones in Fig. 5: the agreement is very good up to 400 K, where Vos, van Hinsberg, and Schouten measure a melting pressure slightly lower than we do. However, this difference remains in the combined uncertainty of the two experiments.

It was found that the melting line of helium from the lower fcc-hcp-liquid triple point up to 24 GPa could be well represented by the Simon law:[11]

$$P = 1.6067 \times 10^{-3} T^{1.565}. \quad (3)$$

The present measurements show no evidence of a triple point on the melting curve. Figure 5 shows that Eq. (3) cannot represent the melting data at high pressure. Furthermore, we were unable to fit the present and previous data with a Simon equation that would respect the accuracy of the different experiments. We show in the discussion that the de-

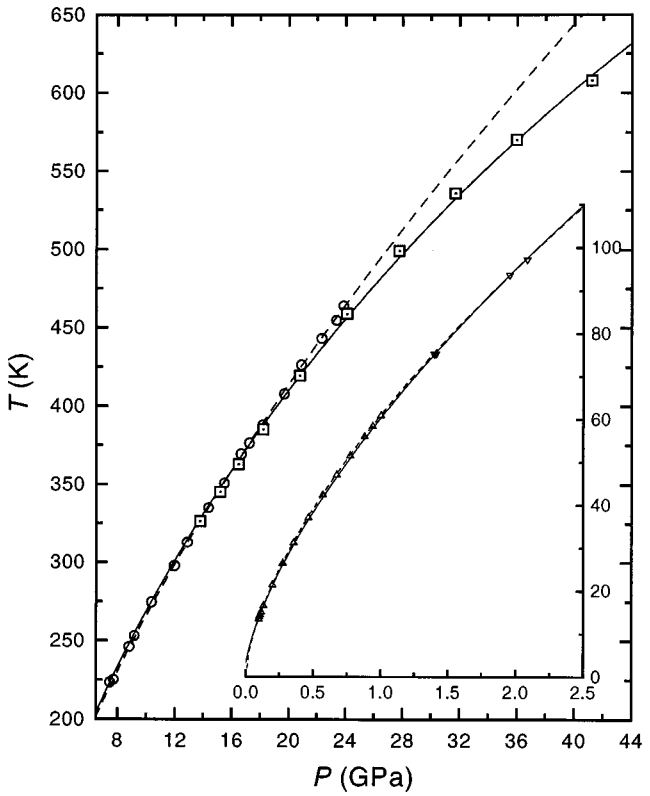

FIG. 5. Melting curve of helium 4. ⊡: this work; ○: Ref. 11; △: Ref. 13; ▽: Ref. 37; ——: Kechin fit to this work $T=T_0(1+\Delta P/0.1259)^{0.6672}\exp(-3.9\times10^{-3}\Delta P)$ with $T_0=15.06$ K and $\Delta P=P-0.1135$ GPa; ––: Simon fit to experimental data up to 24 GPa ($P=1.6067\times10^{-3}T^{1.565}$) (Ref. 11).

viation from the Simon-type behavior might be related to the $\exp(-\alpha r)$ form of the repulsive part of the pair potential of helium. A better fit is obtained when the form proposed by Kechin is used:[12]

$$T=T_0(1+\Delta P/a)^b\exp(-c\Delta P) \tag{4}$$

with $\Delta P=P-P_0$, $T_0=15.06$ K, and $P_0=0.1135$ GPa representing the coordinates of the triple point. This form was derived from a second-order development of the Clausius-Clapeyron equation, whereas the Simon law is a first-order approximation. A least-square fit of the helium melting data gives $a=0.1259$ GPa, $b=0.6672$, and $c=3.9\times10^{-3}$ GPa^{-1}. We note, however, that this fit is not totally satisfactory since the low-pressure measurements of Crawford and Daniels[13] are not reproduced within the accuracy of their experiment.

It has been observed for a long time that the family of the rare (noble) gases satisfies well the law of corresponding states, that is to say, when expressed in reduced units, the thermodynamic properties of the elements of this family are very similar. Application of this law requires that the systems in comparison (i) obey classical statistics and (ii) are well modeled by a pairwise interaction of the form $\phi(r)=\epsilon f(r/\sigma)$, where $f(x)$ is a universal form. Whereas at low density, helium (and in a lesser degree, neon) is very different from the heavier rare gases because of the importance of the quantum effects, at high pressure and temperature, quantum effects are less important and can be treated as a perturbation. Condition (1) is then satisfied. Furthermore, the thermodynamic properties of helium, neon, and argon are well described at high density by an effective pair potential of the exponential-6 form whose stiffness parameter α is very similar from one system to the other: $13.0<\alpha<13.2$. This indicates that the properties of the three elements ''correspond.'' In order to test this, the following relations may be used that scales the presently measured melting points of helium onto the neon or argon temperature and pressure scales:

$$T(\mathrm{He}\rightarrow X)=T_{\mathrm{He}}(\epsilon_{\mathrm{He}}/\epsilon_X), \tag{5}$$

$$P(\mathrm{He}\rightarrow X)=P_{\mathrm{He}}(\sigma_{\mathrm{He}}/\sigma_X)^3(\epsilon_{\mathrm{He}}/\epsilon_X). \tag{6}$$

In the expressions above, X stands for Ne or Ar, and ϵ, σ respectively, represents the energy and position of the well minimum of the exponential-6 potentials.[14] Their values are: $\epsilon=10.8$, 42, 122 K and $\sigma=2.9673$, 3.18, 3.85 Å, respectively, for ^{4}He, Ne, and Ar. As an example, a temperature of 600 K and a pressure of 40 GPa in ^{4}He correspond respectively to $T=2330$ K and $P=126$ GPa in Ne and $T=6780$ K and $P=207$ GPa in Ar. The results of these calculations are plotted in Figs. 6(a) and (b) and compared to the calculations of the melting of Ne[15] and Ar[16] using the exponential-6 potentials. The agreement is good and thus supports the validity of the principle of corresponding states in this range of reduced densities.

C. Melting curve of H_2O

The high-pressure properties of H_2O have important issues in geophysics, astrophysics, chemistry, and condensed-matter physics. Certainly, the knowledge of the melting curve is important for models of the interior of some planets and satellites such as Ganimede. Also, it is predicted that the liquid and solid phases should exhibit an increasing ionicity with pressure. This change would be gradual and continuous in the liquid, as inferred from shock-wave experiments,[17,18] whereas in the solid it could well be discontinuous, that is to say, related to some new high-pressure superionic phase, as predicted by theoretical works.[19] This hypothetical superionic phase between the solid and the ionic liquid could push the melting line to much higher temperatures.

We performed five runs to measure the melting curve of H_2O, in the stability domain of ice VII. The first runs were limited to a temperature of 650 K along the melting curve because the sample of SrB_4O_7:Sm^{2+} (the pressure sensor) was dissolved by water around this P-T range. This problem was solved as explained in Sec. II. Eventually, we could cover the range 356–750 K in temperature, corresponding to pressures between 2.2 and 13.1 GPa. In total, 150 melting

TABLE II. Experimental melting points of ^{4}He determined in this work (T_m in K, P_m in GPa).

T_m	326.2	345.1	362.8	385.1	419.4	459	499	535.7	570	608
P_m	13.8	15.2	16.5	18.2	20.8	24.1	27.8	31.7	36.0	41.2

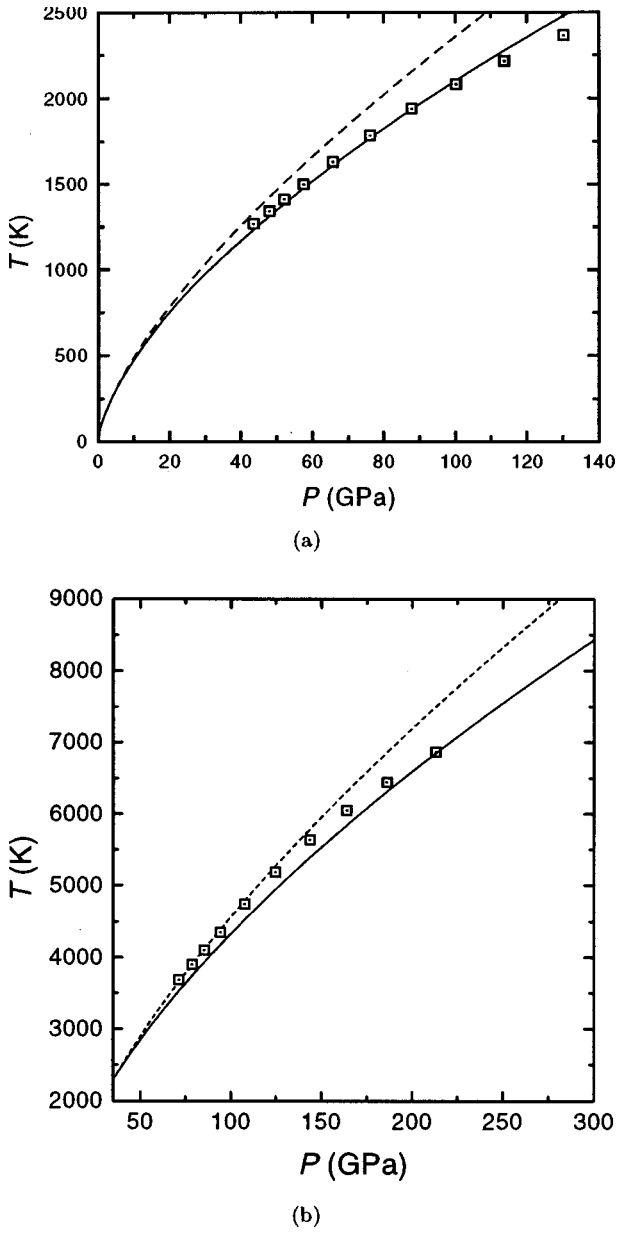

FIG. 6. Melting curve of neon and argon as obtained by applying the corresponding state principle to the present determination of the ^{4}He melting points (dotted squares). (a) Neon; (b) argon. The straight lines represent calculations based on the exponential-6 potentials (Refs. 15 and 16). The dashed lines are the Simon fits to the experimental data.

points were measured, that are gathered in Fig. 7 and Table III. The reproducibility of these measurements is very good, as inferred from the weak dispersion of the data points. The experimental uncertainty is estimated to be ± 0.05 GPa and ± 5 K up to 600 K, increasing to ± 0.15 GPa and ± 10 K at the highest temperatures.

The melting temperature of ice VII is a monotonic increasing function of pressure in the studied range. A least-square fit to a Simon equation gives

$$P = 2.17 + 1.253[(T/354.8)^{3.0} - 1] \quad (7)$$

with a standard deviation of 0.05 GPa. This relation reproduces our whole data set within the experimental uncertainty.

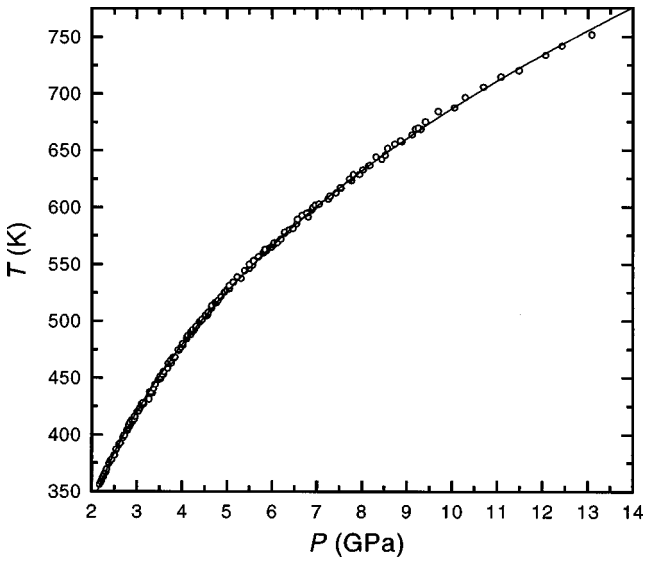

FIG. 7. Melting curve of H_2O (ice VII). The experimental data are represented by circles, the line is a Simon fit to the data: $P = 2.17 + 1.253[(T/354.8)^{3.0} - 1]$.

The coordinates of the triple point VI-VII-liquid were taken as (2.17 GPa, 354.8 K), which represents an average of the values given in the literature. We do not observe a variation of the melting curve that could imply a change in the solid nor the liquid behavior, such as an increase of the ionicity discussed above.

In Fig. 8 we compare our results to previous determinations of the melting curve of ice VII. The first measurements, dating back to 1937, were carried out by Bridgman up to 3.9 GPa.[20] Melting was then detected by the displacement of the piston in the Bridgman press. Other experiments were performed by Pistorius *et al.*[21] with an opposed anvil apparatus and by Mishima and Endo[22] in a multianvil press. Pistorius *et al.* detected melting of the sample by its change in resistance, whereas Mishima and Endo monitored the resistance change of a manganin wire placed inside the sample. Up to this work, only one experiment had been carried out in a DAC by Fei, Mao, and Hemley.[23] They studied melting by monitoring the disappearance of the 110 peak in the x-ray-diffraction pattern. This way, they obtained the minimal melting temperatures at about 7, 9, and 15 GPa.

Up to about 550 K, the present melting line agrees very well with those previous studies. However, our results significantly deviate from those of Pistorius *et al.* and of Mishima and Endo above this temperature, the discrepancy increasing up to 8 GPa at 700 K. The samples used by Pistorius *et al.* were a mix of water, αFe_2O_3, and copper sulfate, in order to reduce the electrical resistivity of water to a value they could more easily measure. It has not been proved that such a mix has the same electrical variation through melting as pure H_2O. Furthermore, they estimated pressure from the ratio of the applied load to the contact area between the anvils but the pressure distribution in the sample is unknown and the deformation of the piston leads to an overestimation of the pressure. Mishima and Endo estimated their pressure from precalibrated applied load on the anvils to a few fixed points *at room temperature*. The authors do not give any indications of the validity of this calibration at high temperature. Fei, Mao, and Hemley's results agree pretty

TABLE III. Experimental melting points of H_2O (ice VII) determined in this work (T_m in K and P_m in GPa).

T_m	P_m	T_m	P_m	T_m	P_m	T_m	P_m	T_m	P_m
355.9	2.18	427.1	3.15	490.0	4.20	556.2	5.71	624.5	7.73
358.3	2.21	427.9	3.14	490.7	4.25	556.5	5.71	628.2	7.82
360.6	2.23	431.0	3.27	491.6	4.28	560.0	5.81	628.6	7.95
362.7	2.26	436.6	3.34	492.1	4.24	561.2	5.83	632.5	8.03
364.8	2.29	437.3	3.29	494.1	4.30	562.0	5.89	636.1	8.16
366.9	2.31	437.7	3.32	495.2	4.32	562.6	5.85	636.5	8.18
369.2	2.33	440.5	3.38	499.1	4.40	564.1	5.95	641.9	8.44
374.4	2.39	444.0	3.41	500.5	4.44	564.5	6.00	644.0	8.32
376.5	2.42	448.1	3.49	501.1	4.45	566.8	6.03	645.5	8.53
377.8	2.45	449.1	3.53	504.5	4.56	568.6	6.06	651.6	8.58
381.7	2.51	450.9	3.52	505.0	4.52	568.8	6.12	655.5	8.74
386.7	2.55	452.6	3.59	506.1	4.58	571.8	6.20	657.5	8.90
390.5	2.61	452.8	3.58	507.4	4.58	577.0	6.29	658.1	8.86
392.3	2.64	455.4	3.60	511.3	4.66	577.8	6.29	663.4	9.12
396.9	2.70	458.3	3.68	513.2	4.66	579.8	6.39	668.2	9.32
399.1	2.73	462.4	3.70	515.8	4.74	581.2	6.47	668.7	9.20
403.6	2.79	463.1	3.77	516.3	4.78	585.0	6.55	669.2	9.26
405.3	2.81	465.1	3.76	517.8	4.80	588.9	6.57	674.9	9.42
407.3	2.85	467.3	3.83	521.0	4.87	591.3	6.81	684.1	9.70
408.0	2.82	467.5	3.81	525.1	4.95	592.4	6.67	687.4	10.06
409.8	2.87	467.8	3.85	527.1	5.00	594.6	6.78	696.5	10.30
410.4	2.85	743.9	3.94	528.5	5.06	597.1	6.89	705.5	10.70
411.4	2.91	474.5	3.92	530.8	5.06	599.4	6.92	714.5	11.09
412.6	2.88	476.6	3.98	534.1	5.15	601.4	6.97	720.1	11.49
413.1	2.94	478.8	4.03	537.4	5.32	602.4	7.05	733.4	12.08
415.9	2.96	478.9	4.03	538.8	5.23	607.1	7.25	741.7	12.44
419.8	3.00	479.8	4.02	544.0	5.40	609.5	7.30	751.5	13.09
420.4	3.03	484.1	4.11	545.9	5.50	612.2	7.43		
423.2	3.08	485.5	4.12	549.1	5.57	616.3	7.54		
425.2	3.11	486.9	4.13	549.7	5.51	616.9	7.53		
426.7	3.11	487.6	4.20	552.8	5.60	623.3	7.78		

well with ours up to 650 K but at 700 K, the melting pressures differ by 4 GPa. One should, however, keep in mind that Fei, Mao, and Hemley's experiment only provides a lower limit for the melting temperature.

On the other hand, it may be suspected that the present determination was made erroneous by the observed reaction between H_2O and SrB_4O_7:Sm^{2+} at high P and T. As a matter of fact, this reaction could plausibly change the luminescence properties of the pressure sensor and thus change the pressure reading. However, in that case, one would expect that two measurements of the melting curve performed subsequently on the same sample would give different results. Such a test was carried out between 500 and 650 K, which revealed no significant difference in the two measurements. In summary, the pressure and temperature calibrations were seriously checked in the present study, thus we believe that our results are more reliable than those of the previous works cited above.

D. Melting curve of hydrogen

Hydrogen presents a fascinating evolution with pressure from a molecular quantum solid to a predicted quantum metal at low temperature or to a strongly correlated plasma at high temperature, as recently observed in dynamical experiments. Although it is the simplest element, there is at present a puzzling discrepancy between theory and experiment. Shock-wave experiments can only study the liquid state because of the large temperature elevation inherent to these experiments whereas the DAC studies have been limited up to now to temperatures below 300 K. Performing static measurements at high temperature and hence reducing the gap between static and dynamic experiments could help to resolve some theoretical issues in hydrogen. Also understanding the properties of hydrogen in its hot and dense state has important applications in planetary physics.

Achieving high pressure and high temperatures on a hydrogen sample in a DAC is challenging because of the high reactivity of this element. The major problem encountered during the present experiments was the diffusion of hydrogen into the gasket above certain P-T conditions. Gaskets are usually made of metallic materials such as tungsten or rhenium, for their large yield strength and ductility are key ingredients to reach high pressures. But in the case of hydrogen, the use of any metal is problematic because of its

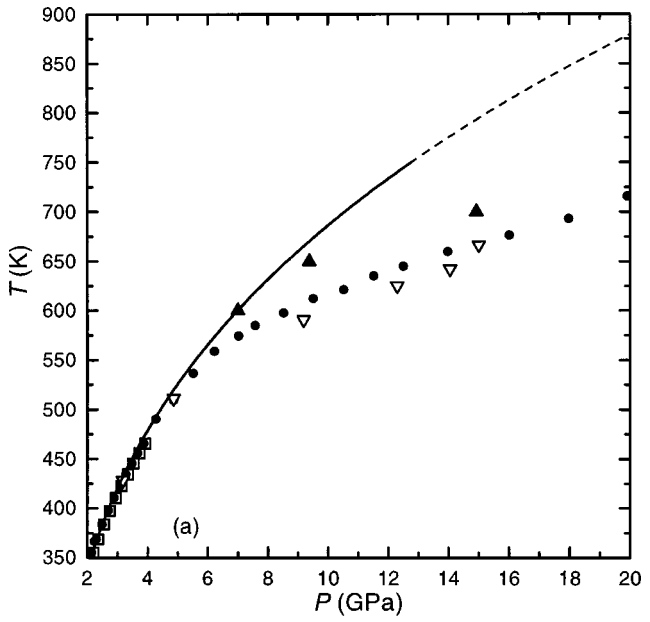

FIG. 8. Comparison between present and previous determinations of the melting curve of H_2O. Full line: this work; dashed line: Simon fit to this work [Eq. (7)]; □: Ref. 20; ●: Ref. 21; ▽: Ref. 22; ▲: Ref. 23.

embrittlement by hydrogen. This solubility is pressure and temperature dependent but all metals are expected to react with hydrogen at high enough pressure and/or high enough temperatures.

Although this phenomenon is well known in a general manner, few works are available that provide a detailed description of it. We have therefore adopted a trial-and-error approach by testing several gasket materials that we believed would be good candidates for our experiments. Table IV gathers the tested materials and the *P-T* conditions at which we observed a strong diffusion of the sample into the gasket. We note that these conditions are just indicative as our goal was to select a material that would allow us to reach higher pressures along the melting curve, not to characterize the process of embrittlement. The metal which appeared to be the most resistant is gold. We also tried to use NaCl which is given in the literature as a hydrogen sealant. However, this gasket could only sustain 12 GPa at 470 K. Extension of this work is clearly dependant on the finding of a better hydrogen sealant gasket material.

TABLE IV. Tested gasket materials for the H_2 experiments. The conditions at which strong diffusion of the sample into the gasket was observed are indicated.

Gasket materials	*P* (GPa)	*T* (K)
BeCu	11	450
Cu	24	300
Al	9	560
Pb	12	500
W	7	510
Re-W	10	550
Au	15	530
NaCl	12	470

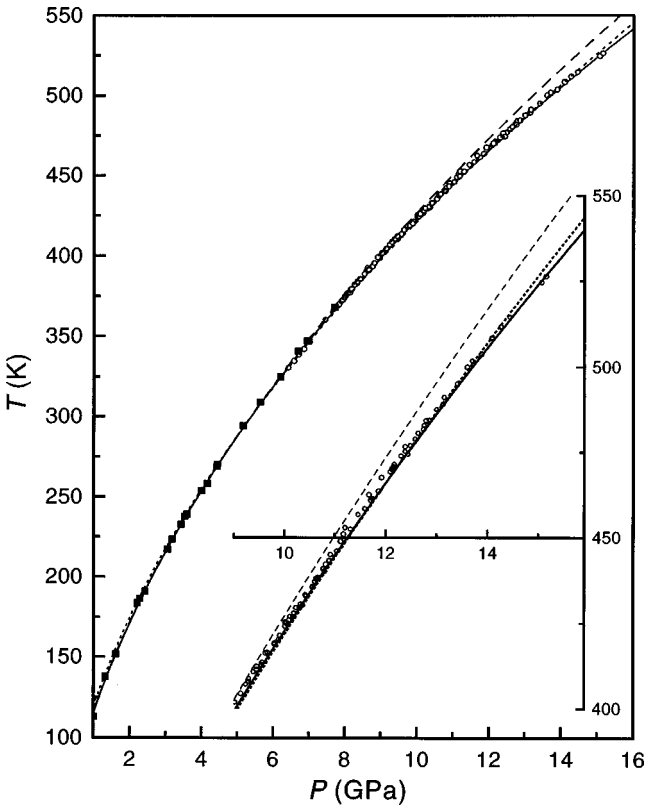

FIG. 9. Melting curve of H_2. Circles: this work; squares: Diatschenko *et al.* (Ref. 24); full line: Kechin fit to this work, $T=T_0(1+P/0.0286)^{0.589}\exp(-4.6\times10^{-3}P)$ with $T_0=14.025$ K, dashed line: Simon fit to Diatschenko *et al.*'s data, $P=2.31\times10^{-4}T^{1.7627}-0.0052$; dotted line: Simon fit to this work and to Diatschenko *et al.*'s data: $P=1.63\times10^{-4}T^{1.824}$.

Figure 9 and Table V gathers the results of four runs, one of them using a BeCu gasket and the three others using a gold gasket. There is no observable difference in the results obtained with either kind of gasket materials, showing that the reaction of hydrogen with the gasket does not contaminate the sample, at least in a measurable proportion. Our measurements range from 6.4 to 15.2 GPa, corresponding to melting temperatures between 330 and 530 K. This almost doubles the pressure range achieved by the latest reported study.[24] The several runs overlap on a wide range, and it can be observed that the measurements were always reproduced within the experimental uncertainty, which is estimated to be better than ±3 K and ±0.05 GPa.

The present results agree very well with those of Diatschenko *et al.*[24] in the overlap region ($330<T<373$ K). These authors proposed the following Simon law to fit their melting data:

$$P=-0.05149+1.702\times10^{-4}(T+9.689)^{1.8077}. \quad (8)$$

This law is plotted in Fig. 9. It is seen to increasingly deviate from the experimental curve: the difference rises up to 0.6 GPa at 530 K, which is well outside the experimental uncertainty. We attempted to fit our results and those of Diatschenko *et al.* with a Simon equation and obtained as the best fit

$$P=1.63\times10^{-4}T^{1.824}. \quad (9)$$

TABLE V. Experimental melting points of H_2 determined in this work. T_m in K and P_m in GPa.

Au gasket						BeCu gasket	
T_m	P_m	T_m	P_m	T_m	P_m	T_m	P_m
330.5	6.42	425.3	10.02	469.3	12.10	373.9	7.98
334.6	6.58	426.7	10.18	470.0	12.13	375.0	8.01
338.6	6.71	426.8	10.12	470.2	12.13	376.1	8.04
342.0	6.86	429.4	10.31	470.4	12.17	376.9	8.07
346.3	7.02	430.2	10.37	470.7	12.16	377.4	8.14
360.3	7.45	430.5	10.33	471.3	12.17	378.8	8.15
366.9	7.69	432.9	10.43	473.9	12.31	379.3	8.17
367.7	7.72	433.2	10.42	474.4	12.44	379.4	8.19
367.9	7.74	435.4	10.56	475.2	12.39	382.2	8.27
369.1	7.81	435.6	10.56	476.6	12.39	384.0	8.35
370.0	7.84	437.1	10.61	477.0	12.49	385.7	8.43
371.8	7.90	437.8	10.63	478.9	12.58	388.8	8.54
372.6	7.94	438.3	10.66	480.6	12.65	391.3	8.67
374.5	8.00	440.8	10.77	481.7	12.76	393.4	8.78
379.0	8.18	442.2	10.82	482.9	12.76	395.6	8.82
382.4	8.27	443.3	10.89	484.3	12.80	399.1	8.92
385.4	8.41	445.0	10.91	484.4	12.86	401.8	9.03
385.7	8.44	446.0	11.05	487.5	13.00	404.3	9.15
390.4	8.59	448.9	11.11	489.1	13.14	407.0	9.25
391.3	8.65	449.4	11.19	491.1	13.16	408.6	9.30
392.5	8.63	451.0	11.17	495.0	13.41	410.6	9.40
407.9	9.30	452.4	11.31	499.9	13.61	412.2	9.46
411.3	9.47	452.9	11.20	501.7	13.71	416.1	9.64
412.6	9.55	456.7	11.46	503.7	13.89	420.1	9.89
413.4	9.57	458.5	11.59	508.2	14.10	424.1	10.03
416.4	9.67	461.0	11.71	508.4	14.09	424.4	10.07
418.7	9.81	461.5	11.74	511.7	14.27	425.9	10.10
419.1	9.81	462.5	11.68	514.4	14.45	427.9	10.20
421.3	9.92	463.6	11.86	524.6	15.07	429.4	10.23
425.1	10.05	467.5	11.93	526.3	15.16	440.1	10.80
						441.6	10.87
						442.5	10.89
						457.6	11.53

The use of a four parameter relation as in Eq. (8) does not improve the results. Figure 10(a) shows the difference between the experimental melting points and those calculated with Eq. (9). The difference grows outside the experimental uncertainty and shows systematic trends. Hence a Simon law is not adequate to represent the melting curve of H_2. By contrast, the use of the Kechin equation (see Sec. III B) gives a very good fit:

$$T = T_0(1 + P/0.0286)^{0.589} \exp(-4.6\times 10^{-3} P), \quad (10)$$

where $T_0 = 14.025\,\mathrm{K}$ is the melting point at $P = 0$. The fit reproduces very well all the published experimental melting points, from about $P = 0$ to $P = 15\,\mathrm{GPa}$. As shown in Fig. 10(b), the difference between calculated and experimental points is always lower than the experimental uncertainty, and appears randomly dispersed around zero.

IV. DISCUSSION: MELTING CURVES AT VERY HIGH PRESSURE

As we mentioned above, the knowledge of the melting curves of the systems presently studied, and especially of He and H_2, is not only of fundamental interest but is also relevant for the modeling of the interior of the giant planets. Unfortunately, the present extension in pressure and temperature of the experimental determination remains far below the conditions existing in these planets, and one has still to rely on theoretical predictions. For each system studied above, we have given the best fit to melting laws either of the Simon or Kechin forms. These equations give a convenient analytical form to represent the data and should *a priori* be used only in the *P-T* range covered by experiment. But since they are also often used for purpose of extrapolation of the experimental data, the question whether this extrapolation is justified is an important issue. Several authors have tried to find a theoretical justification to these laws. It was shown in the 1960s that for systems interacting via a $1/r^n$ interaction,

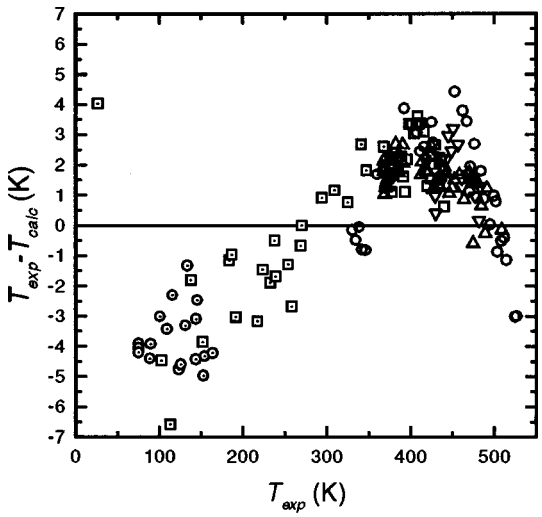

(a)

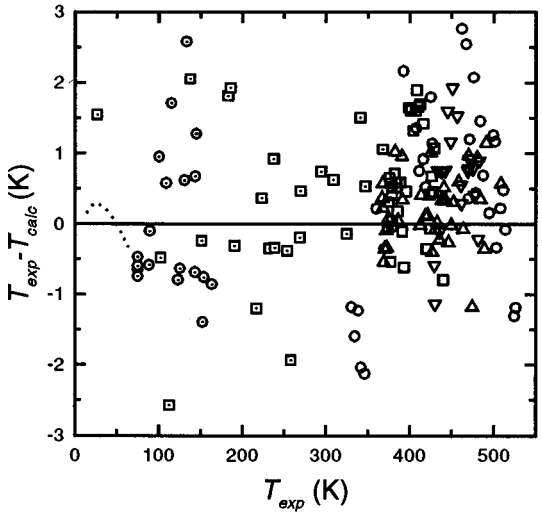

(b)

FIG. 10. Residue plots of the fits to the melting data on H_2. (a) Simon fit: $P=1.63\times10^{-4}T^{1.824}$; (b) Kechin fit: $T=14.025(1+P/0.0286)^{0.589}\exp(-4.6\times10^{-3}P)$. Dotted circles: Ref. 38, dotted squares: Ref. 24; dotted line: Simon fit from Ref. 39; all other symbols represent the data obtained in this work.

the melting line was exactly of the Simon form (see, for example, Ref. 25). This accounts for example for the Simon-type behavior of the melting line of argon at low density since the interactions are then well modeled by a Lennard-Jones potential. However, with increasing density, the $1/r^n$ potential turns out to be too stiff to represent the interaction of real systems and the melting line is expected to deviate from the Simon law. In the family of the rare gases, this deviation should be observed in He at a lower pressure than in the others since, at a given pressure, helium probes a higher reduced density. Indeed, we observed such a deviation here for ^{4}He, whereas the melting line of argon is still well represented by a Simon law at the highest pressure achieved so far (using the corresponding state principle as explained in Sec. III B, the deviation would be expected in Ar at about 6000 K and 150 GPa).

To address semiquantitatively the behavior of the melting

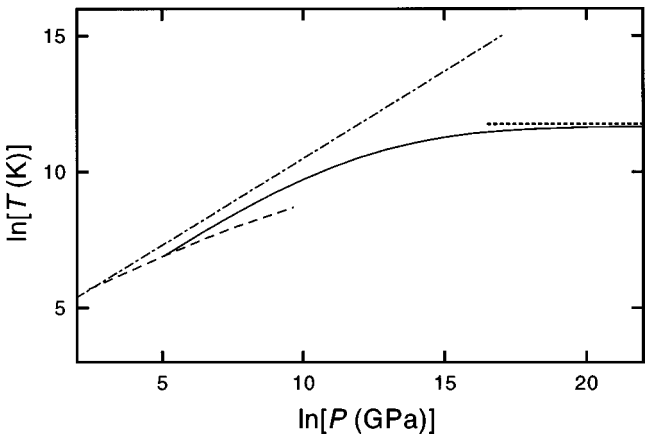

FIG. 11. Melting of ^{4}He at very high density. Full line: qualitative model described in the text; dashed line: Calculations from Ref. 26; dashed-dotted line: Simon fit to experimental data to 24 GPa (Ref. 15).

curve of He at very high pressure, we can use the following phenomenological model: as mentioned above, the repulsive part of the pair potential of He is well modeled by the form $\exp(-\alpha r)$. Since at high density, the properties of the crystal are dominated by interactions among nearest neighbors of distance R_1, it is possible, by neglecting the thermal effects, to relate the evolution of the melting curve to the one of a $1/r^n$ potential in which n depends on the density. We so define for a given density d an effective n by

$$n=-\left(r\frac{d\ln\phi(r)}{dr}\right)_{R_1}=\alpha R_1. \tag{11}$$

Pressure is then given by $P=-dU/dV$, with $U=zA\exp(-\alpha R_1)$, and z: number of nearest neighbors. Then,

$$P=\frac{\sqrt{2}}{3}zA\alpha\frac{\exp(-\alpha R_1)}{R_1^2}. \tag{12}$$

For a $1/r^n$ interaction, the melting pressure is given by[25] $P=aT^{1+3/n}$, so that $dP/P=(1+3/\alpha R_1)dT/T$. By integration, we obtain the system

$$\begin{cases}\ln(T)=-\alpha R_1+\ln(\alpha R_1+3)+C\\ P=\dfrac{\sqrt{2}}{3}zA\alpha\dfrac{e^{-\alpha R_1}}{R_1^2}.\end{cases} \tag{13}$$

In the limit R_1 goes to zero, i.e., P goes to infinity, this model predicts a maximum melting temperature $T=\exp(C)$ whereas the Simon equation leads to a divergence of the melting temperature. Hence for a sufficient variation of R_1, the melting line should deviate from the Simon law, in correspondence with the softening of the potential. Figure 11 compares the evolution of the melting curve as predicted by the Simon law and by the system (13)—for the calculation of the system (13), we use the effective pair potential derived by Young, McMahan, and Ross[26] from band structure based calculations, which extend the exp-6 potential at very high densities. This calculation is also compared to the one of Young, McMahan, and Ross[26] using the same potential: a

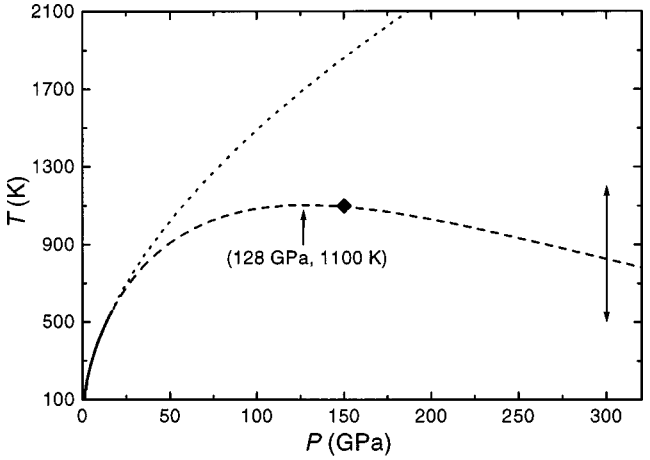

FIG. 12. Melting curve of H_2 according to the extrapolations of the Kechin law [dashed line, Eq. (10)] and to that of the Simon law [dotted line, Eq. (9)]. The full line represents the experimentally determined line. The double arrow indicates the interval within which Hohl *et al.* observed the melting of a H_2 sample in a *ab initio* molecular dynamics simulation (Ref. 28). The diamond represents the point where Pfaffenzeller and Hohl observed a transition from the molecular to the dissociated fluid in a recent *ab initio* molecular dynamics simulation (Ref. 32).

semiquantitative agreement is observed, the difference originating from the thermal effects being neglected in our model.

In the case of H_2, a similar deviation from the Simon behavior due to the softness of the potential is expected. However, this deviation is observed in the present experiments at a lower temperature (about 500 K) than expected. Indeed, the pair potential of H_2 is very similar to that of Ne, and according to the corresponding state principle, the deviation from the Simon law in Ne should occur around 1000 K. This may indicate that a different mechanism tends to stabilize the fluid phase at lower temperature. Some results obtained by recent *ab initio* calculations are interesting in this regard. Alavi, Parinello, and Frenkel,[27] on one hand, studied the evolution of a system of 64 atoms at $T=1000\,\mathrm{K}$, using an extension of the Car-Parinello method at finite electronic temperature, and observed that the system is fluid and strongly diffusive over the whole range of studied densities, i.e., $3.673 \leqslant \rho \leqslant 1.840\,\mathrm{cm}^3/\mathrm{mol}$, corresponding to pressures approximately between 30 and 300 GPa. On the other hand, Hohl *et al.*[28] performed a molecular dynamics simulation using the density functional theory and the local-density approximation, and observe that their sample at 300 GPa becomes very diffusive between 500 and 1200 K. The value of the diffusion coefficient at the latter temperature, $10^{-3}\,\mathrm{cm}^2/\mathrm{s}$, is characteristic of a liquid.

Figure 12 shows the extrapolation of the Simon and Kechin fits to the present experiment on H_2. It can be seen that the melting temperature predicted by the Simon law is well above the estimation given by Hohl *et al.* at 300 GPa. By contrast, the melting temperature given by the Kechin law is consistent with the *ab initio* calculations. This extrapolation extend way above the experimental range and may seem audacious but, still, the coincidence is interesting and, as we showed above, the Kechin law fits very well all the experimental data obtained so far on H_2.

One can also see that according to the Kechin law, the melting temperature of H_2 would present a maximum of 1100 K at 128 GPa. As we shall see, this point seems consistent with the results of the *ab initio* calculations cited above. Let us recall first that this phenomenon has been observed in several systems in which it can be qualitatively explained by a simple model proposed by Rapoport.[29,30] This model supposes that the short-range structure of the liquid present a similar order as that of the solid near the melting line. Then, if a second structure appears in the solid as a high-pressure phase, a second structure, presenting a similar short-range order as that of the high-pressure solid phase may also appear in the liquid phase at lower pressure. The liquid then consists of two phases corresponding to the low- and high-pressure solid phases. Because of the disorder, the transition to the higher density species occurs continuously in the liquid as the density increases, whereas this transition can only occur with a finite jump of volume and structure in the solid. The liquid may thus become denser than the solid in a certain *P-T* range, and the melting curve will then go through a maximum.

This model seems reasonable for a number of species whose melting curve present a maximum. For example, in Te, computer simulations have shown that around the maximum (1.2 GPa, 740 K), the liquid is a mix of fragments of helicoidal chains, reminiscent of the low-pressure solid phase, and of ''metallic'' atoms.[31] With increasing pressure and temperature, the chains dissociate and the proportion of the metallic component increases. At 4 GPa, a structural phase transition occurs in solid Te to a metallic phase and the melting line slope becomes positive again above the triple point.

A similar scenario could well occur in H_2. Indeed, the calculations of Alavi *et al.* show that the fraction of dissociated molecules increases sharply in the fluid above 150 GPa at 1000 K, and in a very recent simulation, Pfaffenzeller and Hohl report a transition to a dissociated fluid phase at about 150 GPa and 1100 K,[32] which is strikingly close to the melting curve maximum predicted by the Kechin law. A number of studies have shown by now that solid H_2 is still molecular at 150 GPa, the molecular to atomic transition being more likely to occur around 600 GPa.[33] It is then reasonable to think that with increasing density, the increasing fraction of dissociated molecules in the fluid may lead to a fluid phase that is denser than the solid. This could also explain why, in the calculations of Alavi *et al.*, the calculated specific volume of the fluid is systematically smaller than that of the solid as measured at 300 K.[27] We mention however that there is a strong disagreement today in the calculated values of the fraction of dissociated molecules between the *ab initio* simulations cited above, and those based on the experimental Hugoniots and free-energy models of H_2:[34] according to the latter, the fraction of dissociated molecules is negligible at $P=150\,\mathrm{GPa}$ and $T \simeq 1000\,\mathrm{K}$.

V. CONCLUSION

We have reported extended experimental determinations of the melting curves of argon, H_2, H_2O, and ^4He to temperatures as high as 750 K. The experiments used a resistively heated diamond anvil cell made out of ceramic materials. Accurate measurements at high pressure and high

temperature could be achieved by the use of an *in situ* metrology based on two luminescence sensors, ruby and $SrB_4O_7:Sm^{2+}$. The precision of this method, of order of 1%, is comparable to the one at room temperature. Measurements of the argon melting line between 300 and 740 K served as a test for these techniques. It was shown that the melting line of argon is still well represented by a Simon equation up to 6.3 GPa. The melting line of ^{4}He was measured up to 41.2 GPa (608 K), which almost doubles the highest pressure achieved so far. We observed that the melting temperature increases faster with pressure than the extrapolation of the Simon fit to the low-pressure data, which we qualitatively explained by the softening of the repulsive interactions with increasing density. Our measurements of the H_2O melting line up to 13.09 GPa (751.5 K) showed large discrepancies with respect to previous determinations at temperatures higher than 550 K. Because we repeated these measurements several times on different samples and because the calibrations in this work were seriously checked and validated by other experiments, we came to the conclusion that those previous works were erroneous. The melting temperature of H_2O is a regular monotonous function of pressure in the studied range and can be very well represented by a Simon law. Finally, we almost doubled the pressure range achieved in previous measurements of the melting line of H_2, and extended it to 15.16 GPa (526.3 K). Further extension was prohibited by diffusion of the sample into the gold gasket, which was the more resistant gasket among the several other ones tested. However, because of the good precision of these measurements, we were able to show that one needs a higher-order approximation law than the Simon equation to fit the melting data. A fit to the Kechin equation gave a very satisfactory result. By comparing our results to *ab initio* calculations, we indicated the possibility of a maximum melting temperature for H_2 at about 128 GPa and 1100 K. Because these conditions are within reach of today's technology, this point should be a good motivation to carry on this work.

*Electronic address: fd@pmc.jussieu.fr

[1] R. Hemley and N. Ashcroft, Phys. Today **51** (8), 26 (1998).

[2] R. LeToullec, F. Datchi, P. Loubeyre, N. Rambert, B. Sitaud, and T. Thévenin, in *High Pressure Science and Technology*, edited by W. A. Trzeciakowski (World Scientific, London, UK, 1996), p. 54.

[3] R. LeToullec, P. Loubeyre, and J. P. Pinceaux, Phys. Rev. B **70**, 2368 (1989).

[4] R. A. Forman, G. Piermarini, J. Narnett, and S. Block, Science **176**, 284 (1972).

[5] F. Datchi, R. LeToullec, and P. Loubeyre, J. Appl. Phys. **81**, 3333 (1997).

[6] W. Hardy, R. Crawford, and W. Daniels, J. Chem. Phys. **54**, 1005 (1971).

[7] S. M. Stishov and V. I. Fedosimov, Pis'ma Zh. Eksp. Teor. Fiz. **14**, 326 (1971) [JETP Lett. **14**, 217 (1971)].

[8] C.-S. Zha, R. Boehler, D. A. Young, and M. Ross, J. Chem. Phys. **85**, 1034 (1986).

[9] A. P. Jephcoat and S. P. Besedin, Philos. Trans. R. Soc. London, Ser. A **354**, 1333 (1996).

[10] P. Loubeyre, Phys. Rev. Lett. **58**, 1857 (1987).

[11] W. L. Vos, M. G. E. van Hinsberg, and J. A. Schouten, Phys. Rev. B **42**, 6106 (1990).

[12] V. V. Kechin, J. Phys.: Condens. Matter **7**, 531 (1995).

[13] R. K. Crawford and W. B. Daniels, J. Chem. Phys. **55**, 5651 (1971).

[14] F. H. Ree, in *Simple Molecular Systems at High Density*, edited by A. Polian, P. Loubeyre, and N. Boccara (Plenum, New York 1988), p. 153.

[15] W. L. Vos, J. A. Schouten, D. A. Young, and M. Ross, J. Chem. Phys. **94**, 3835 (1991).

[16] A. B. Belonoshko, High Press. Res. **10**, 583 (1992).

[17] A. C. Mitchell and W. J. Nellis, J. Chem. Phys. **76**, 6273 (1982).

[18] N. C. Holmes, W. J. Nellis, and W. B. Graham, Phys. Rev. Lett. **55**, 2433 (1985).

[19] C. Cavazzoni, G. L. Chiarotti, S. Scandolo, E. Tossati, M. Bernasconi, and M. Parrinello, Science **283**, 44 (1999).

[20] P. W. Bridgman, J. Chem. Phys. **5**, 964 (1937).

[21] C. W. Pistorius, M. C. Pistorius, J. P. Blakey, and L. J. Admiraal, J. Chem. Phys. **38**, 600 (1963).

[22] O. Mishima and S. Endo, J. Chem. Phys. **68**, 4417 (1978).

[23] Y. Fei, H. K. Mao, and R. J. Hemley, J. Chem. Phys. **99**, 5369 (1993).

[24] V. Diatschenko, C. W. Chu, D. H. Liebenberg, D. A. Young, M. Ross, and R. L. Mills, Phys. Rev. B **32**, 381 (1985).

[25] J. P. Hansen and I. R. McDonald, *Theory of Simple Liquids* (Academic, New York, 1976).

[26] D. A. Young, A. K. McMahan, and M. Ross, Phys. Rev. B **24**, 5119 (1981).

[27] A. Alavi, M. Parinello, and D. Frenkel, Science **269**, 1252 (1995).

[28] D. Hohl, V. Natoli, D. M. Ceperley, and R. M. Martin, Phys. Rev. Lett. **71**, 541 (1993).

[29] E. Rapoport, J. Chem. Phys. **46**, 2891 (1967).

[30] E. Rapoport, J. Chem. Phys. **48**, 1433 (1968).

[31] J. Hafner, J. Phys.: Condens. Matter **2**, 1271 (1990).

[32] O. Pfaffenzeller and D. Hohl, J. Phys.: Condens. Matter **9**, 11 023 (1997).

[33] P. Loubeyre, R. LeToullec, D. Hausermann, M. Hanfland, R. J. Hemley, H. Mao, and L. Finger, Nature (London) **383**, 702 (1996).

[34] M. Ross, Phys. Rev. B **58**, 669 (1998).

[35] P. H. Lahr and W. G. Eversole, J. Chem. Eng. Data **7**, 42 (1962).

[36] J. D. Grace and G. Kennedy, J. Phys. Chem. Solids **28**, 977 (1967).

[37] R. L. Mills, D. H. Liebenberg, and J. C. Bronson, Phys. Rev. B **21**, 5137 (1980).

[38] D. H. Liebenberg, R. L. Mills, and J. C. Bronson, Phys. Rev. B **18**, 4526 (1978).

[39] R. L. Mills and E. R. Grilly, Phys. Rev. **101**, 1246 (1956).

[40] At room pressure, the total wavelength shift of the line between 300 and 750 K is 0.035 nm, that is two orders of magnitude lower than the shift of the ruby R lines (Ref. 5). We checked that it remains true under pressure by performing isochoric scans in the solid phase.

[41] Larh and Eversole (Ref. 35), and later, Grace and Kennedy (Ref. 36), reported experiments at higher pressure (1.8 and 2.6 GPa, respectively), but these are known to be less reliable than subsequent experiments performed by Refs. 6 and 7.